

# Buncefield investigation

Liquid flow and vapour production

Prepared by the **Health and Safety Laboratory**  
for the Health and Safety Executive 2012

# Buncefield investigation

## Liquid flow and vapour production

**GT Atkinson & SE Gant**  
Health and Safety Laboratory  
Harpur Hill  
Buxton  
Derbyshire  
SK17 9JN

This report on the liquid flow from the overfilled tank leading to the formation of flammable vapour in the Buncefield Incident was prepared for the HSE incident investigation. The purpose of the work was to provide a connection between the loss of containment and the formation of a flammable vapour cloud. Practical and numerical investigations have demonstrated that the bulk of fuel vaporisation and entrainment of air occurred during the cascading of fuel from the top of the tank into the bund.

The work involved the construction of a full scale replica of a section of top of the tank involved at Buncefield and also a full height section of the tank wall. Liquid flow experiments were carried out. The overall liquid flow results in a relatively fine spray, with droplets a few millimetres in diameter. Numerical analysis of heat, mass and momentum transfer (between droplets in the fuel cascade and the air that surrounds them) has shown that the fuel cascade drives a significant downward flow of air. The air is contaminated by high concentrations of light hydrocarbons and is cooled. Final temperatures and concentrations within liquid and vapour are likely to be very close to equilibrium values.

This report and the work it describes were funded by the Health and Safety Executive (HSE). Its contents, including any opinions and/or conclusions expressed, are those of the authors alone and do not necessarily reflect HSE policy.

© Crown copyright 2012

*First published 2012*

You may reuse this information (not including logos) free of charge in any format or medium, under the terms of the Open Government Licence. To view the licence visit [www.nationalarchives.gov.uk/doc/open-government-licence/](http://www.nationalarchives.gov.uk/doc/open-government-licence/), write to the Information Policy Team, The National Archives, Kew, London TW9 4DU, or email [psi@nationalarchives.gsi.gov.uk](mailto:psi@nationalarchives.gsi.gov.uk).

Some images and illustrations may not be owned by the Crown so cannot be reproduced without permission of the copyright owner. Enquiries should be sent to [copyright@hse.gsi.gov.uk](mailto:copyright@hse.gsi.gov.uk).

# CONTENTS

<b>1</b>	<b>INTRODUCTION.....</b>	<b>1</b>
<b>2</b>	<b>CONSTRUCTION OF TANK 912.....</b>	<b>2</b>
<b>3</b>	<b>MODEL TESTS.....</b>	<b>9</b>
3.1	Model 1 – A section of the tank perimeter .....	9
3.2	Model 2 – A full-height section of the tank wall .....	13
3.3	Test with unleaded petrol.....	18
3.4	Overall spray dimensions.....	19
3.5	Summary of results on spray generation .....	20
<b>4</b>	<b>CALCULATION OF VAPORISATION RATES .....</b>	<b>21</b>
<b>5</b>	<b>RESULTS OF VAPORISATION MODELLING .....</b>	<b>22</b>
<b>6</b>	<b>SUMMARY OF CHARACTERISTICS OF VAPOUR (AND RESIDUAL LIQUID) PRODUCED BY FALLING SPRAYS.....</b>	<b>27</b>
6.1	Low liquid overflow rate (550 m <sup>3</sup> /hr).....	27
6.2	High liquid overflow rate (960 m <sup>3</sup> /hr).....	27
<b>7</b>	<b>CONCLUSIONS.....</b>	<b>29</b>
<b>8</b>	<b>APPENDIX: DETAILS OF THE CFD MODEL .....</b>	<b>30</b>





# EXECUTIVE SUMMARY

## Objectives

Blast and fire damage at Buncefield followed ignition of an extensive low-lying cloud rich in hydrocarbons. This cloud developed during overfilling of a tank with unleaded petrol. The purpose of this report is to explain the connection between the loss of containment and the generation of a combustible cloud.

## Main Findings

Practical and numerical investigations have demonstrated that the bulk of fuel vaporisation and entrainment of air occurred during the cascading of fuel from the top of the tank into the bund.

Roughly half of the liquid released flowed out over the edge of the tank and formed a freely falling spray. The other liquid was initially deflected by an inclined plate and ran down the tank wall. At an elevation of around 9 m above the bund, liquid running down the wall hit a circumferential stiffening girder (wind girder) and was projected out, away from the tank, passing through the cascade of liquid from above.

The overall liquid flow results in a relatively fine spray, with droplets a few millimetres in diameter.

Numerical analysis of heat, mass and momentum transfer (between droplets in the fuel cascade and the air that surrounds them) has shown that the fuel cascade drives a significant downward flow of air. The air is contaminated by high concentrations of light hydrocarbons and is cooled. The outputs of this analysis, i.e. the velocity and composition of the vapour flow driven by the falling liquid spray, can be used as inputs in large scale dispersion modelling.

The hydrocarbon mixture entering the vapour cloud that surrounds the tank is fuel rich. The volume flow is sufficient to establish a cloud of depth 1.6 – 2 m deep over the area affected by the vapour cloud explosion (VCE). CCTV records of the cloud suggest that the final volume of the cloud was somewhat increased by entrainment as the cloud flowed away from the source. Areas around the periphery of the cloud may have had concentrations close to the stoichiometric ratio and this would have clearly been a factor in increasing the power of the resulting VCE in these areas.

Increases in liquid flow into the tank at the end of the period when it was overflowing may also have contributed to variations in the cloud concentration between areas close to the tanks (where burning was slow and fuel rich) and the periphery of the cloud where there was a powerful explosion.



# 1 INTRODUCTION

On the morning of 11<sup>th</sup> December 2005 there was a large explosion and fire at the Buncefield fuel depot. This appears to have been caused by a release of petrol from one of the large storage tanks, which was overfilled. The liquid released from the tank formed a dense, low-lying vapour cloud, which spread out across the fuel depot and neighbouring areas before it was ignited. After the fire HSL was requested by David Painter (a Specialist Inspector in HSE's Hazardous Installations Directorate) to investigate several aspects of the incident.

The objective of this report is to provide information on the liquid flow from the top of the tank, the break up of this liquid as it cascaded down to the ground and the generation of a flammable vapours.

During the early hours of 11<sup>th</sup> December 2005 unleaded petrol was arriving at HOSL West Tank 912 on the Buncefield site via the Thames/Kingsbury (T/K South) pipeline from Coryton at rate shown in Table 1. This data has been supplied to the authors by the HSE Investigation Team.

Time	Flow rate (thousands of litres/hr)	Flow rate (kg/min)	Flow rate (kg/s)
3:00	546	6370	106
4:00	541	6311	105
5:00	553	6451	107
5:53	714	8330	139
5:54	926	10,800	180
5:57	955	11,150	186
5:58	920	10,700	179
6:00	890	10,400	173
6:01	860	10,030	167

**Table 1:** Flow rate into Tank 912 prior to the incident

The initial explosion occurred at 6:01. For approximately 24 minutes prior to the explosion CCTV records show a thick mist flowing out of the bund surrounding Tank 912. This suggests that that at approximately 5:30 Tank 912 began to overflow.

The purpose of this report is examine:

1. The fate of liquid that ran out of Tank 912.
2. The generation of an airflow heavily contaminated with fuel vapours – the volume flux, temperature and chemical composition of the flow are of particular interest.

## 2 CONSTRUCTION OF TANK 912

The overall design and dimensions of Tank 912 are shown in Figures 1, 2 and 3.



**Figure 1:** Upper part of Tank 912

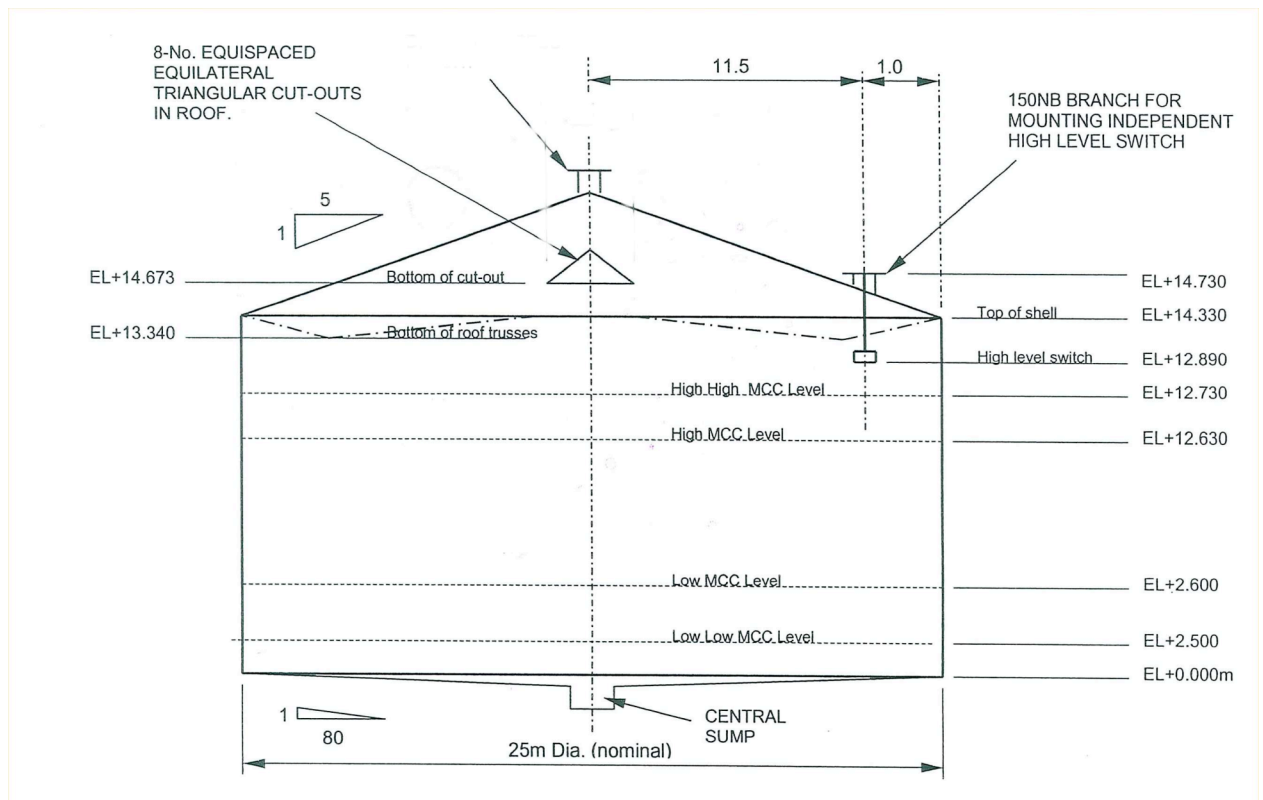


**Figure 2:** Tank 912 overall dimensions



**Figure 3:** View of Tanks 912 (left) and Tank 915 (right) in Bund A

Eight breather vents are located on the top of the tank – these are of particular importance as this is where liquid finally flowed out of the tank. Details of these vents and their shrouds are shown in Figures 4, 5 and 6. Tank details have been supplied to the authors by Robert Nixon - a Specialist Inspector working with the HSE Investigation Team.

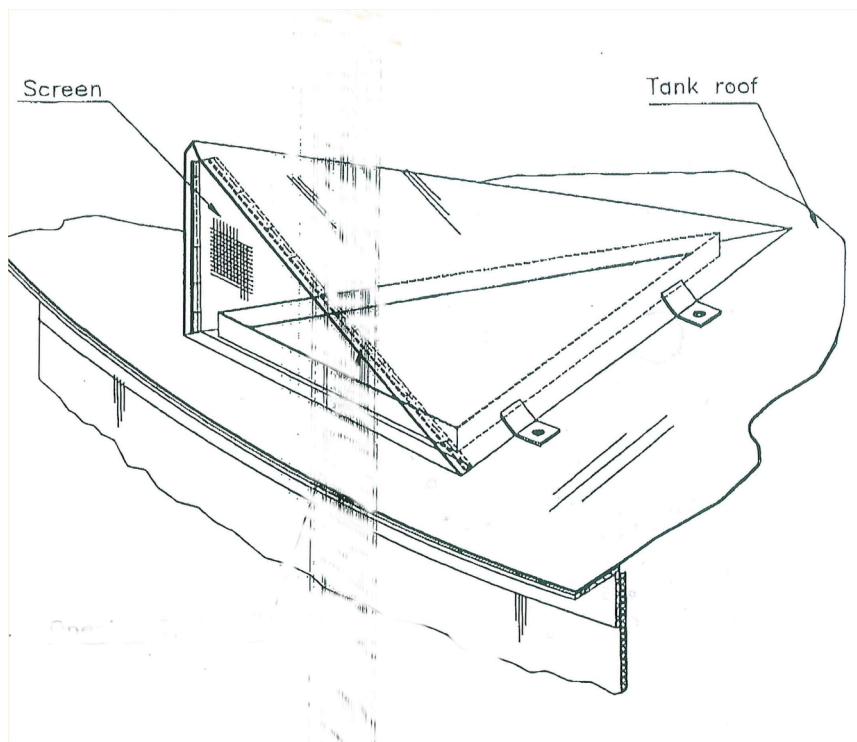


**Figure 4:** Schematic of layout of breather vent and shroud. The distance from the breather to the edge of the tank is much larger than shown – in proportion to the vent size.



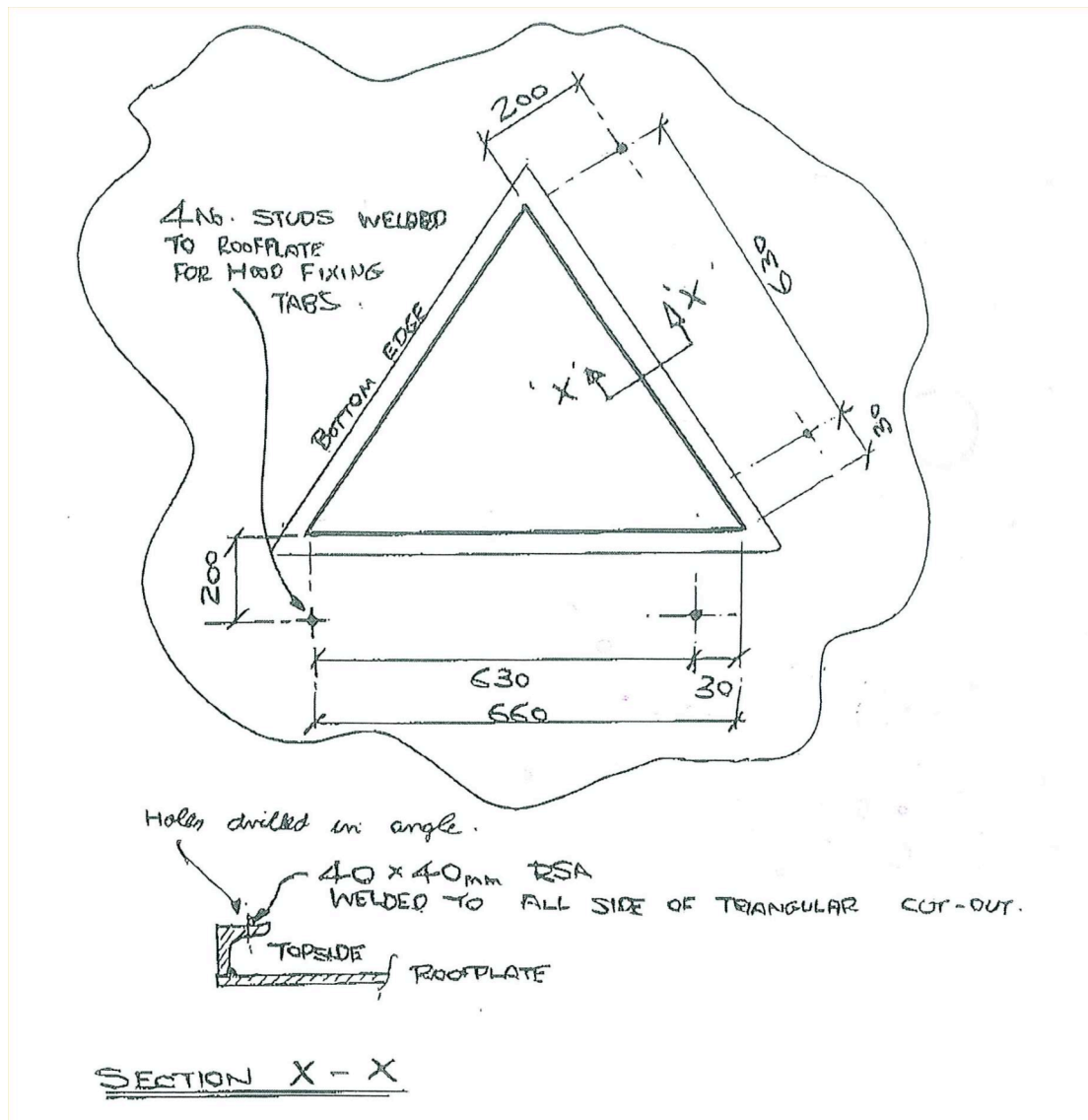


**Figure 5:** Dimensions of breathing vents

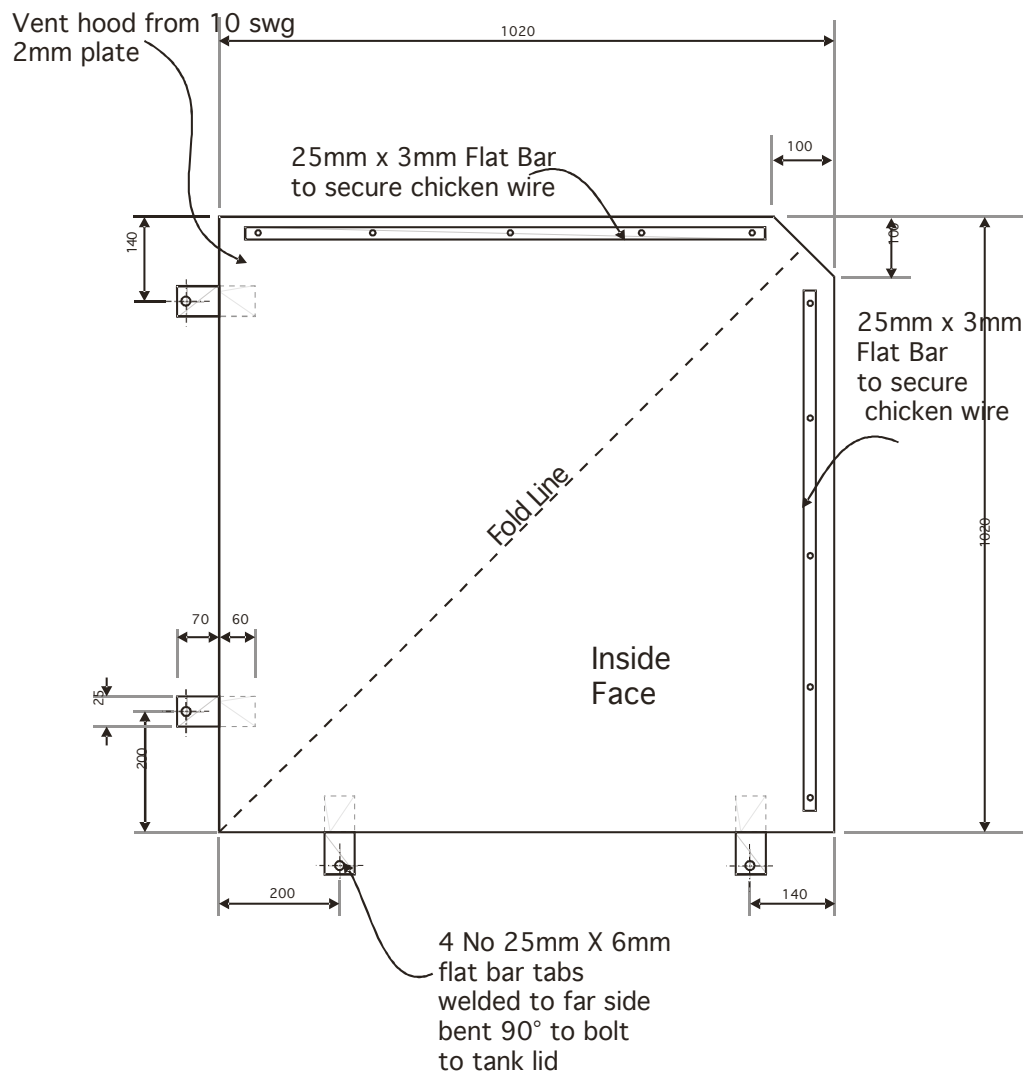


**Figure 6:** Construction of breather vent shroud

The tank is fitted with a deflector plate at the edge of the roof. The purpose of this plate is to redirect sprinkler water flowing down the roof back onto the walls of the tank. This would improve the efficiency with which sprinklers could cool tank walls in the event of a bund fire.

During the overflow of fuel from the tank breather vents, the deflector plate would have redirected a proportion of the flow back towards the tank wall. However, the flow rates per unit length of tank perimeter were much greater during the overflow than would have been the case in the event of sprinkler operation. This meant that a proportion of the liquid flowing down from the vents would have flowed over the top of the deflector plate. This type of liquid flow is illustrated in Figure 7 (See Section 3 for details of experiments). The partitioning of liquid (between that overtopping the deflector plate and that redirected back into contact with the wall) is a key factor in determining the efficiency of dispersion of the liquid into a fine spray and the consequent vaporisation.

The design of the deflector plate is shown in Figure 8.



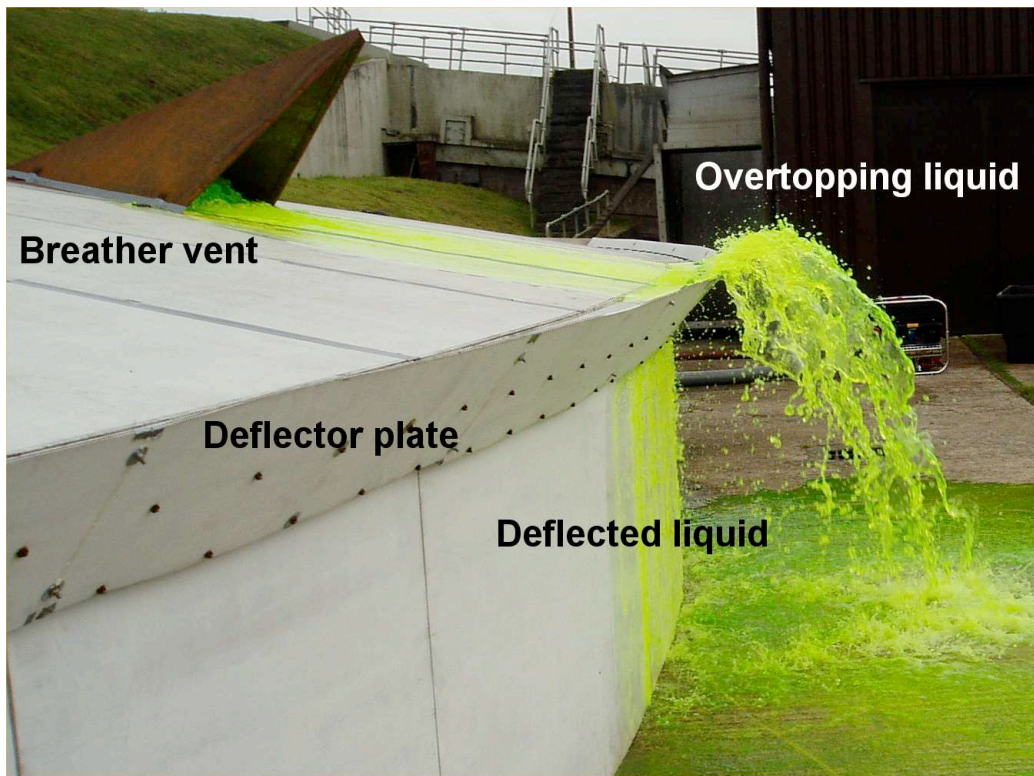


**Figure 7:** Liquid flow from a breather vent and over the edge of a (full-scale) model of part of Tank 912.

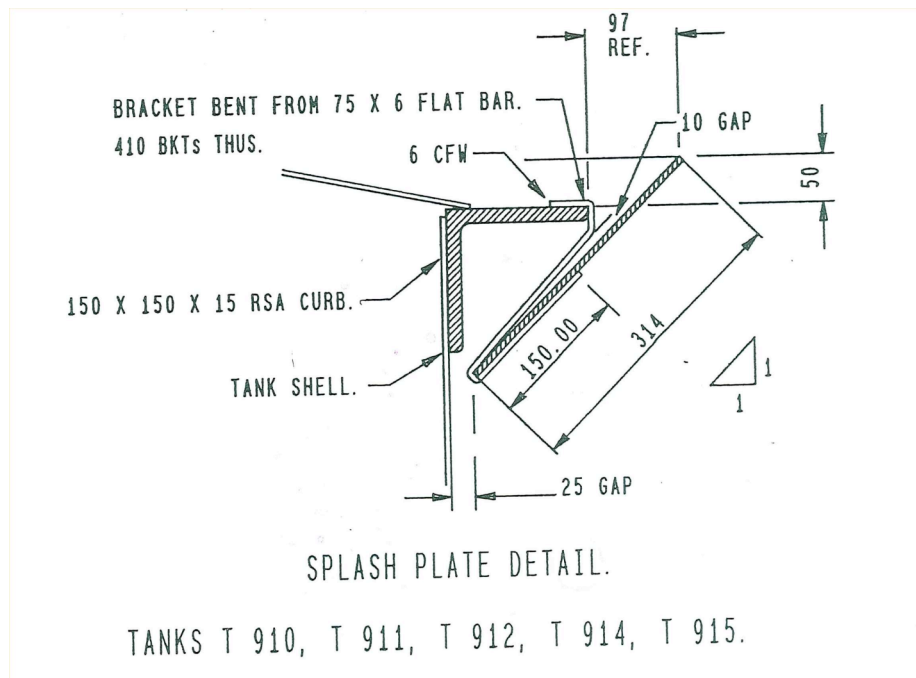
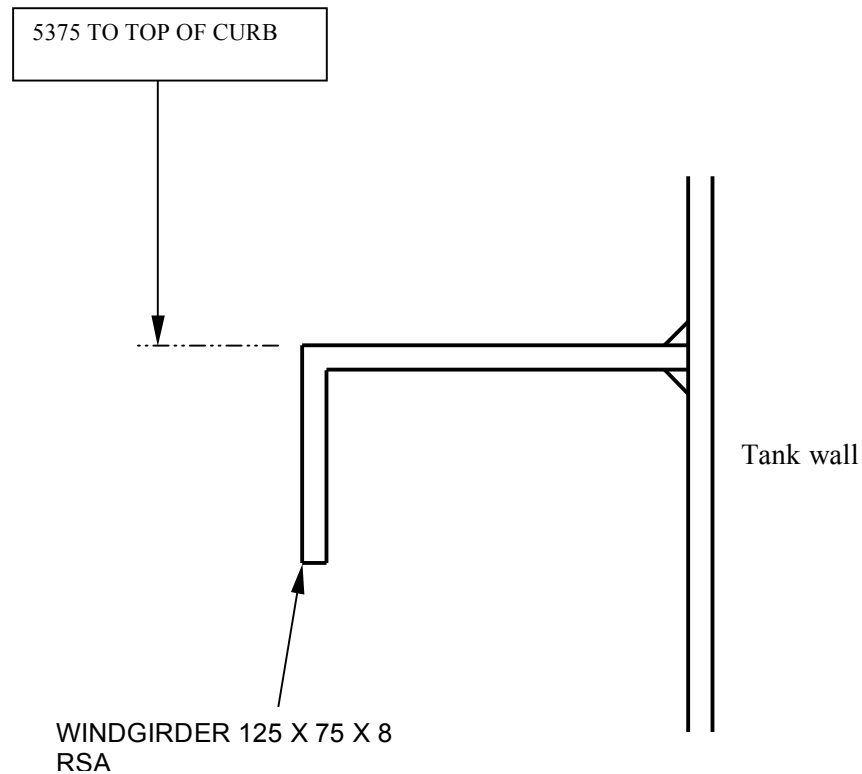


**Figure 8:** Detail of construction of deflector plate  
(n.b. as built the brackets were irregularly spaced around the tank at intervals 500-1000mm)

An additional detail of tank construction of particular significance in determining liquid flow and spray formation is the wind girder. This is an angle section fully welded to the tank wall to stiffen the tank against side loads in windy conditions – see Figures 1 and 3. Details of the location and dimensions of this girder are shown in Figure 9. The wind girder is approximately 9 metres above the bund surface.



DETAIL OF WINDGIRDER

TAKEN FROM McTAY DRAWING  
1805/022 REV A

**Figure 9:** Details of wind-girder

Liquid flowing rapidly down the wall of the tank strikes this girder and is deflected outwards. At flow rates relevant to this incident the detachment of the liquid flow from the wall by the wind girder appears to be complete. The flow is illustrated in Figures 10 and 11 – taken from full-scale model tests (see Section 3).



**Figure 10:** Detachment of wall flow (4 l/m/s) striking the wind-girder in a model  
(n.b there is no simultaneous flow overtopping the deflector plate in this case)

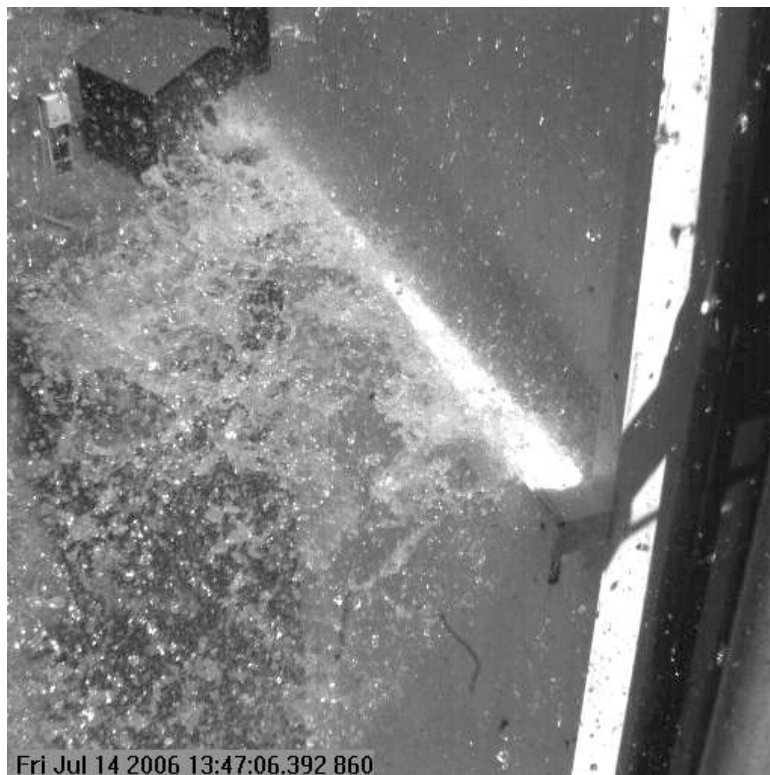


**Figure 11:** Frame from high-speed video of the area around the wind-girder.  
(n.b. in this case there is a simultaneous overtopping flow of 7 litres/m/s)

### 3 MODEL TESTS

#### 3.1 MODEL 1 – A SECTION OF THE TANK PERIMETER

Two models have been made to represent different sections of Tank 912 - at full scale. The portion of the tank represented by Model 1 is shown in Figure 12.



**Figure 12:** Typical section of Tank 912 represented by Model 1

Care was taken to reproduce the detail of the deflector plate – especially its dimensions and location relative to the edge of the tank.

Brackets obstruct a small proportion of the gap between the deflector plate and tank rim. These brackets therefore slightly reduce the amount of liquid running down through the gap and back onto the tank wall. Sensitivity tests suggest that the wall flow (for a given total flow) was roughly proportional to the length of tank rim that is unobstructed – as is to be expected.

The model of tank 912 was constructed from drawings of the tank which showed 80% of the perimeter unobstructed. Physical evidence of tank 912 recovered from the site some time after the event revealed that as built, the tank had approximately 90% of the tank perimeter unobstructed. The model results are therefore likely to underestimate the flow of liquid back to the wall by around 12%.

Water was used as the test fluid in all cases – for practical reasons. The depth of the flow between the centre of the vent and the tank rim is relatively large and the shear force between the tank top and the fluid above is fairly small compared with the component of gravity inclined along the surface. Even for water, the liquid running from the centre of the vent regains a high proportion of its original height after it hits the deflector plate.

The dynamic viscosity of petrol is roughly half that of water. The flow down the tank top would be slowed somewhat less by friction than in these tests on water. Minor increases in the proportion of the liquid overtopping the deflector plate (for a given total flow) could be expected if petrol had been the test fluid. These differences are likely to be minor compared with the huge changes in the degree of overtopping caused by changes in total flow.

Typical results for water flow rates of 22.3 litres/second and 41.3 litres/second are shown in Figures 13 and 14. For comparison the flow rates **per vent** during the Buncefield overflow are shown in Table 2:

Time	Flow rate (thousands of litres/hr)	Flow rate per vent (litres/second)
3:00	546	19
4:00	541	18.8
5:00	553	19.2
5:53	714	24.7
5:54	926	32.2
5:57	955	33.2
5:58	920	32
6:00	890	30.9
6:01	860	29.9

**Table 2:** Flow rates **per vent** during the Buncefield.

It is clear that the width of the flow overtopping the deflector plate is much greater at the higher flow rate. The width of the flow down the wall caused by the deflector plate also increases but only marginally.

The low flow rate illustrated corresponds roughly to the overflow rate during most of the overflow at Buncefield. The proportion of the tank wall wetted by liquid during the Buncefield overflow would have been around 30% between 05:30 and 5:52, probably



increasing to around 33% between 05:53 and 05:57. This estimate is based on a linear interpolation between the widths observed for flow rates of 22.3 and 41.3 litres/s.

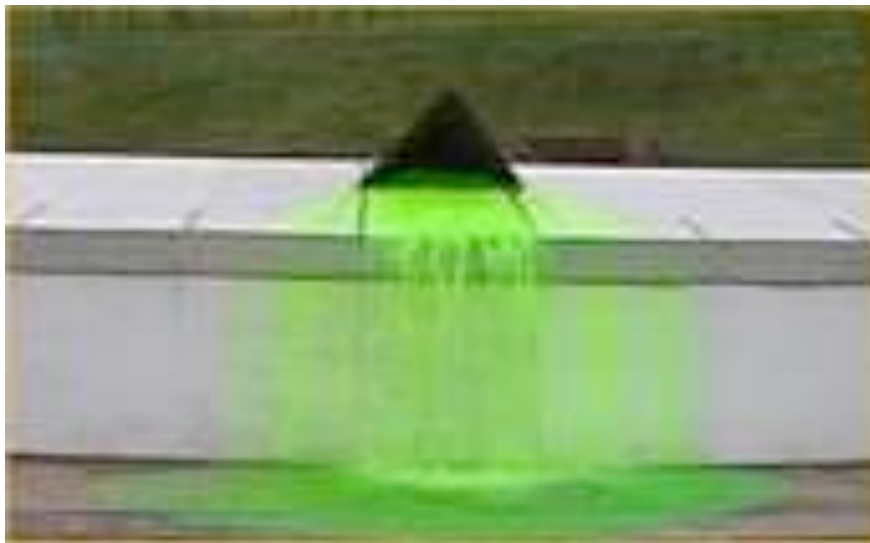


**Figure 13:** Water flow from vent 22.3 litres/second



**Figure 14:** Water flow from vent 41.3 litres/second

Measurements of the proportion of liquid that overtopped the deflector plate were made – by collecting this flow in large plastic tanks. A summary of results is shown in Table 3. These results are displayed graphically in Figure 15.

Test	Volume (litres/sec)	Overtopping flow (litres/sec)	Wall flow (litres/sec)	% Overtopping flow	% Wall flow
1*	4.83	0	4.83	0	100
2	12.9	4.48	8.43	34.7	65.3
3	22.3	10.6	11.7	47.5	52.2
4	41.3	28.7	12.6	69.5	30.5

\* The flow rate was adjusted until overtopping of the deflector plate just stopped

**Table 3:** Summary of results on partitioning of liquid

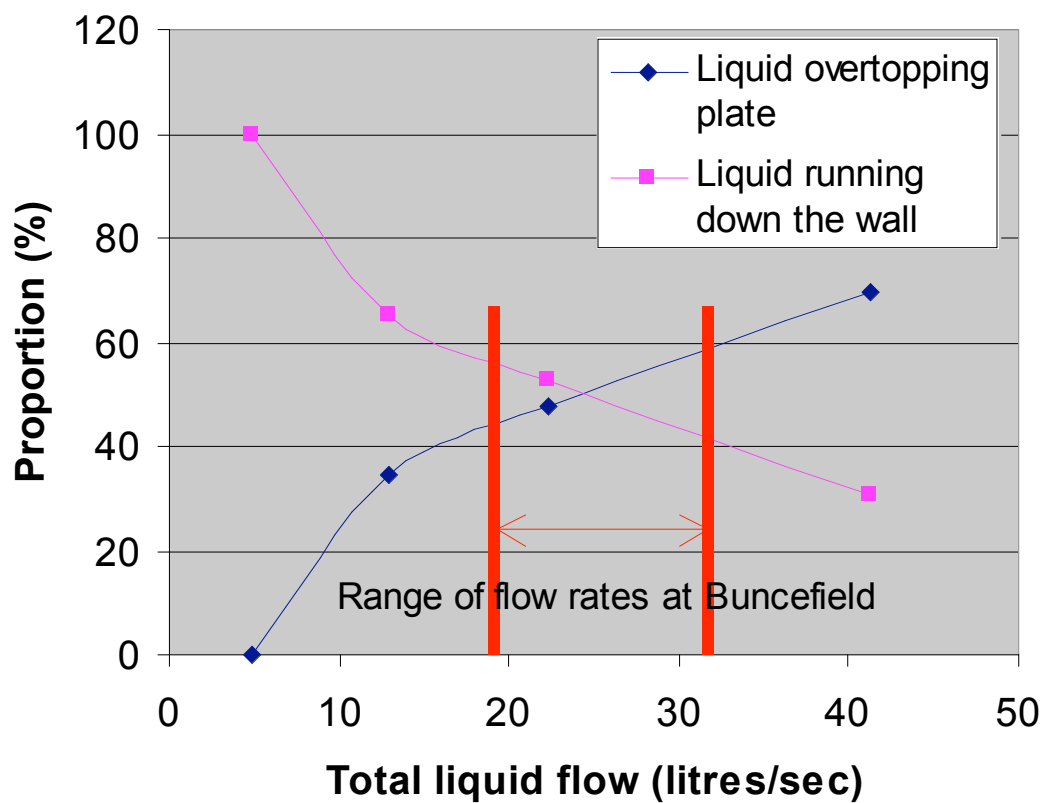


**Figure 15:** The partitioning of a liquid release into an overtopping flow and one directed down the wall. The range of liquid releases during the Buncefield incident is shown.

### 3.2 MODEL 2 – A FULL-HEIGHT SECTION OF THE TANK WALL

The portion of the tank represented by Model 2 is shown in Figure 16.



**Figure 16:** Typical section of Tank 912 represented by Model 2

The purpose of tests with this second model was to investigate the dispersion of falling liquid into a finely divided spray.



Most experiments were carried out using water. A comparison between water and a petrol sample from the Thames/Kingsbury (T/K south ) pipeline from Coryton at Buncefield (under seal A02438) is described later in this report.

Both long exposure photography and high-speed video were used to study the spray structure. In some cases it is difficult to justify or even adequately illustrate conclusions drawn from the videos in a written report such as this. Copies of videos are available from HSE.

The tests demonstrated the fundamental importance of the wind girder in determining dispersion both of the wall flow – which is perhaps to be expected – and of the overtopping flow. This second effect was unexpected and arises because the wall flow is projected rapidly through the falling overtopped flow - Figure 17.



**Figure 17:** Intersection of sprays from the deflector plate (7 l/m/s) and wind-girder (4 l/m/s)

The collision of wall and overtopped flows is particularly effective at triggering droplet break up – especially in the overtopped flow. At the level of the wind-girder the fluid in the overtopped flow still includes a proportion of relatively large droplets (>10mm diameter). Such droplets would rapidly disintegrate in a quiescent flow, because drag forces on the drop would overcome surface tension. In the falling overtopped flow there is a co-flow of gas, drawn down by the accelerating liquid. The slip velocities between liquid and vapour are fairly low.

This low-slip velocity regime is violently disrupted by the flow from the wind girder. Although droplets may miss each other as they pass at right angles, the associated vapour flows cannot intersect – both must be deflected. If the vapour co-flow surrounding large drops

is deflected the droplets soon find themselves in high slip conditions and catastrophic disintegration into hundreds of small pieces occurs.

High-speed video of the collision region shows that hardly any large falling drops make it through the zone where wind-girder and overtopped flows collide.

The effect this has on the character of the spray can be illustrated with long-exposure still photographs (1 second exposure). The wall flow in each frame in Figure 18 is 4 litres/metre/s. The image on the left also has an overtopped flow of 7 litres/second/metre.

Figure 17 shows that the apparent density of a simple falling spray declines steadily in this type of image. This is because droplets move further apart as they speed up. On the other hand in Figure 18 the apparent density at the point marked X is greater than in the spray above the collision zone. The effect of collision is to fragment both sprays and make both more visible.

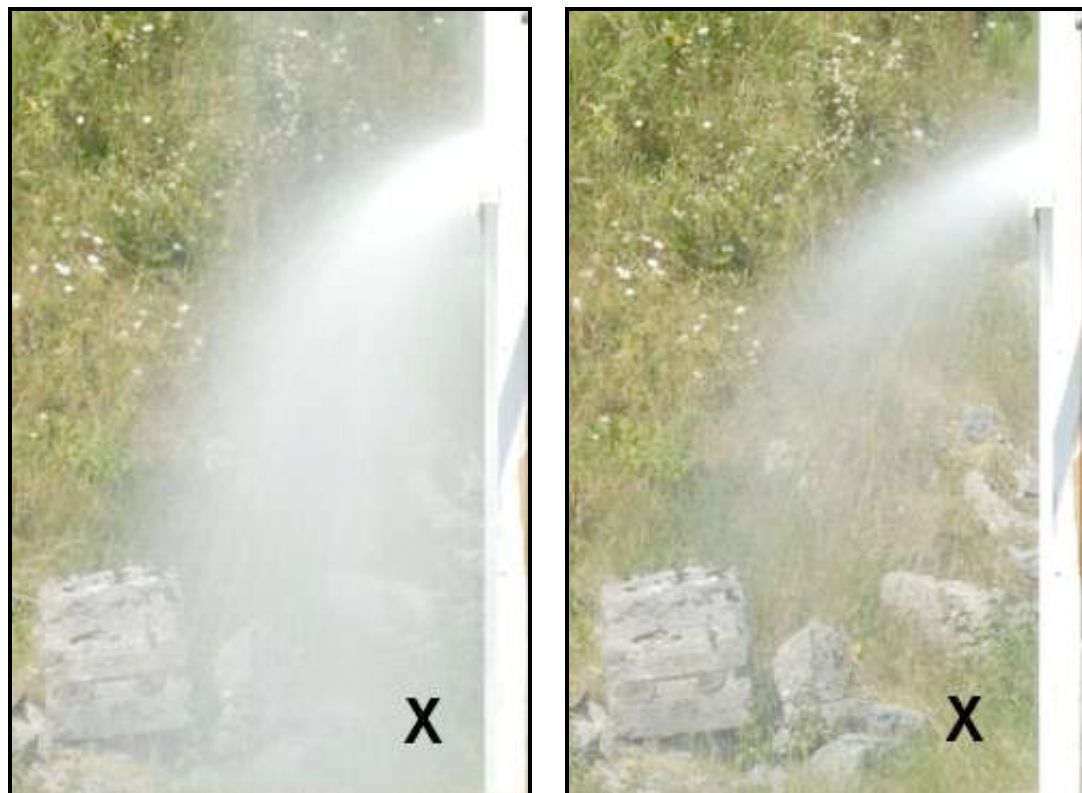


**Figure 18 (left):** Wall (4 l/s/m) and overtopped (7 l/s/m) flows

**Figure 18 (right):** Wall (4 l/s/m)

Some high-speed images are shown in Figure 19. In the area covered by the close-up there are relatively large filaments of liquid moving slowly outward and downward from the wind girder. These appear to change relatively slowly between frames. A high-speed droplet from the overtopping flow is shown (marked with an arrow) undergoing the initial stages of fragmentation. The fragmentation of scores of droplets is clearly visible on a high-speed video (1000 frames/s) covering 1 second of flow. The still images shown are unfortunately not clear.

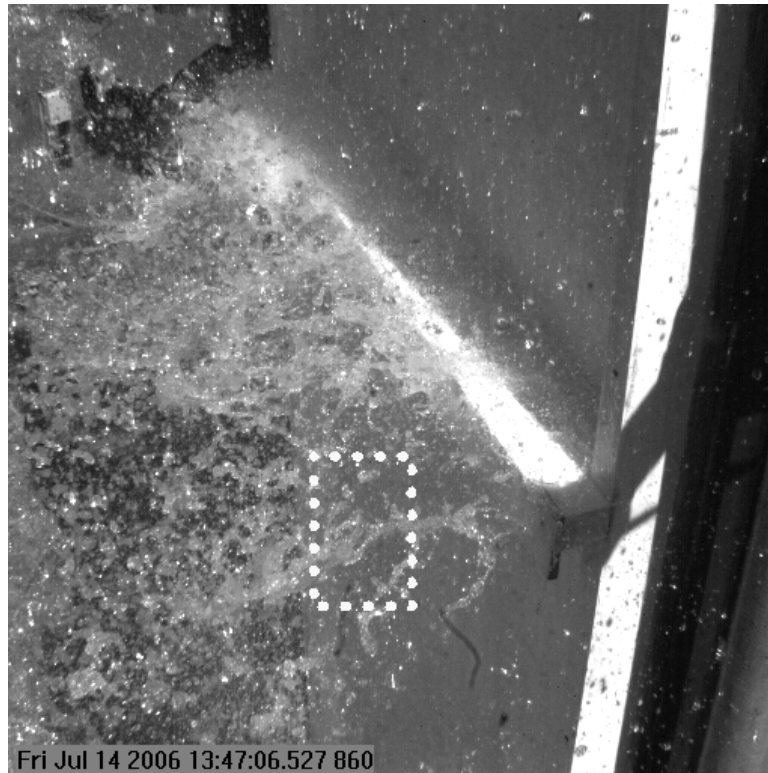


**Figure 19a:** Area shown in close up

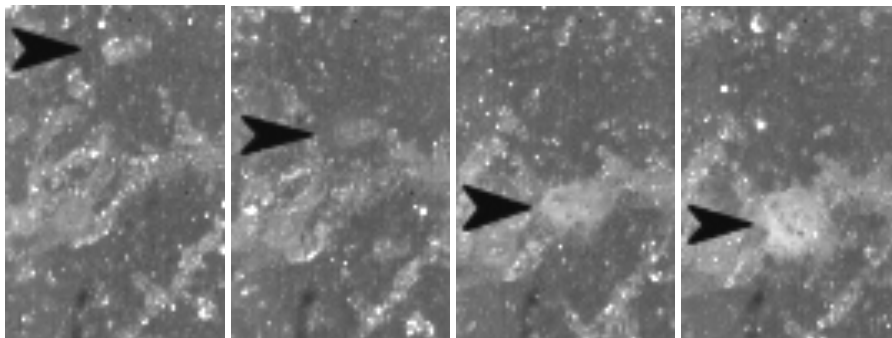


**Figure 19b:** Relative timing of frames 0, 5, 10 and 12 ms

Figure 20 shows droplet break-up near the bottom of an overtopping spray. The spray has been videoed at a height of 2m above the ground. The spray is less dense and clearer still images can be obtained. Some larger droplets have survived the fall but as the gas co-flow approaches the ground it slows and the relative velocity between droplets and gas increases. This causes an increase in the shear forces on the droplets, which then fragment.

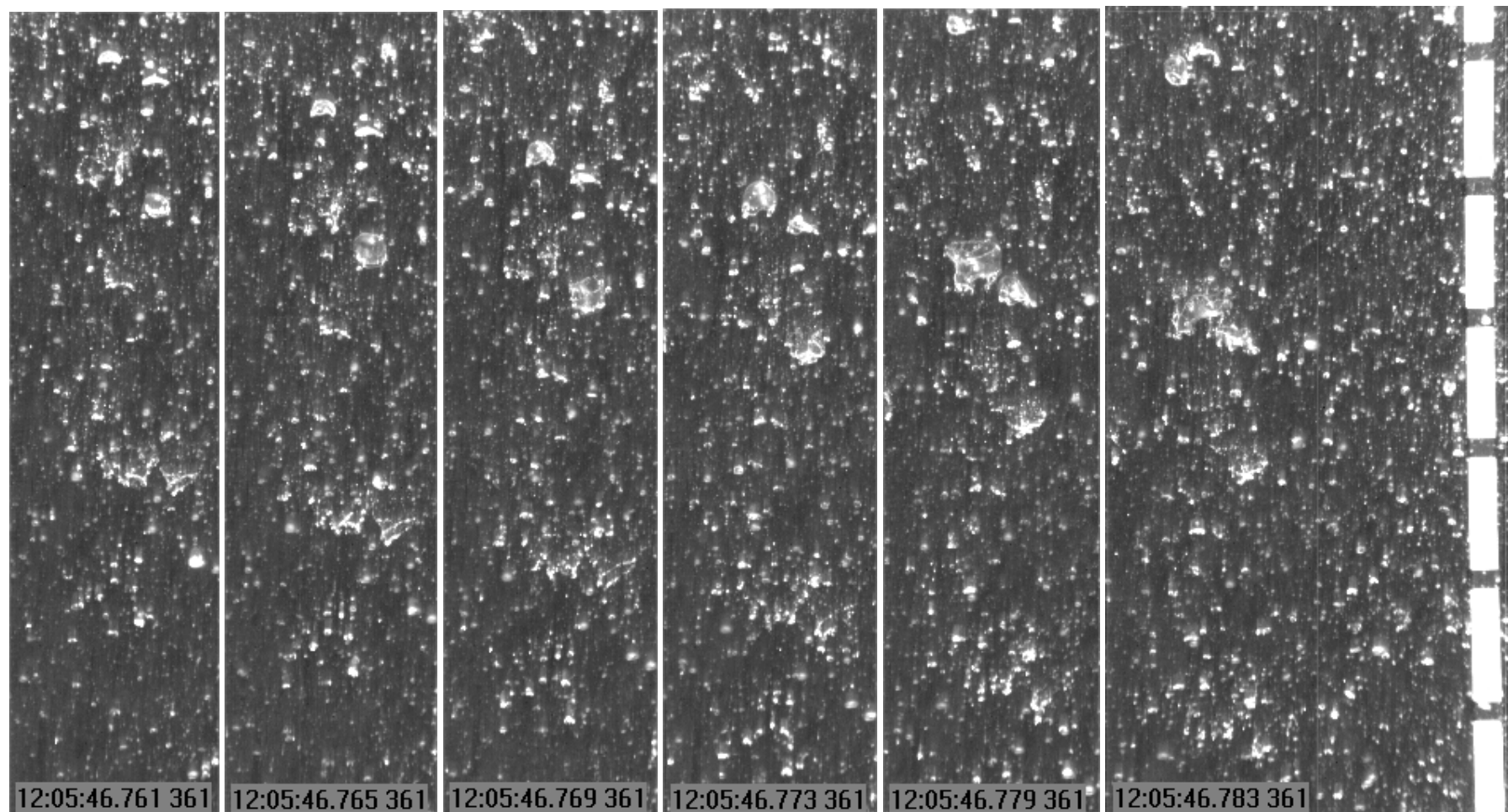


**Figure 20 :** A sequence of video frames as an overtopped spray approaches the floor (no wall flow)  
The interval between dark marks on the right is 100mm.

### 3.3 TEST WITH UNLEADED PETROL

The surface tension and density of water and hexane (at 20°C) are compared in Table 4. Surface tensions of other major components of petrol are fairly similar to hexane.

	Surface tension (N/m)	Density (kg/m3)
<b>Water</b>	0.0727	998
<b>Hexane</b>	0.0184	667

**Table 4:** Surface tension of water and hexane

The parameter that controls the breakup of droplets moving through a gas is the Weber number.

$$We = \frac{\rho V^2 D}{\sigma}$$

In this formula:  $\rho$  is the air density,  $V$  is the velocity difference between droplet and air,  $D$  is the droplet diameter and  $\sigma$  is the surface tension.

If the Weber number exceeds a critical value droplets will fragment. If the Weber increases sharply (to well above this critical value) the droplet break-up will be catastrophic; forming a very large number of tiny droplets.

For an isolated falling droplet the terminal slip velocity is a strong function of the droplet diameter. This is less true for droplets that move into cross flows. In this case, the characteristic perturbation in slip velocity is primarily a function of the speeds of the intersecting flows. All droplets experience roughly similar perturbations – whatever their size.

If this were the case one would expect the limiting size of surviving droplets to be inversely proportional to surface tension. Since the surface tension of petrol is of order 4 times less than water, this would mean that a perturbation in velocity that led to the break-up of all water droplets with a diameter greater than 4mm, would fragment all petrol droplets with a diameter greater than 1mm.

In principle the differences between the surface tension of water and petrol could be significant in determining the fineness of the spray produced and an experiment was carried out to investigate this effect practically.

The experiment involved separate releases of 5 litre samples of water and petrol from a 50 mm (i.d.) diameter pipe. The rate of release was driven by a controlled flow of compressed gas and was equal in each case (~3 litres/second). The spray fell freely, well away from solid obstacles. There was no intersecting spray at an intermediate level.

High-speed video was taken of the resulting spray, 14 metres below the release point.

The video results are hard to summarise as still images. Figure 21 compares the sprays of water and petrol droplets observed.



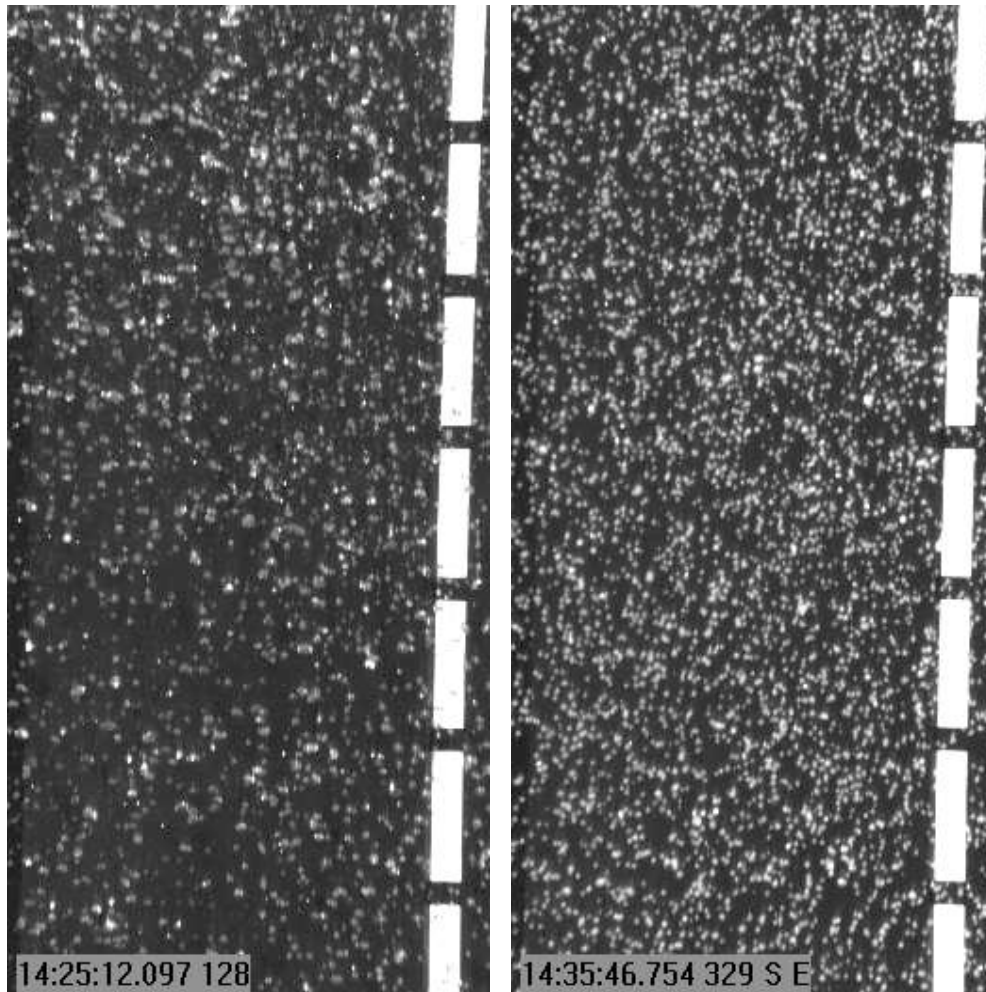


**Figure 21:** Pulse releases of water (left) and petrol (right).  
Observations made 14m below the plane of release

The droplets in the water spray are typically larger and more variable in diameter. The characteristic size of droplets in the petrol spray was in the range 2-3 mm (diameter). It is possible that smaller droplets may have been produced if the spray had suffered a collision with a perpendicular flow e.g. a horizontal spray projected from the wind girder.

The sound made by the impacting petrol spray was much softer than the familiar percussive sound of a water flow from elevated leak. Recordings were not made of these sounds.

### 3.4 OVERALL SPRAY DIMENSIONS

The thickness of the spray, i.e. the distance it extends from the wall, increases rapidly immediately below the wind girder – see Figure 10, 17 and 18. The rate of spread of the spray then declines rapidly and a few metres below the wind-girder the spray thickness is approximately constant. When the wall and over-topping flows are similar to those during a 550 m<sup>3</sup>/s overflow, the spray extends to a distance of approximately 1.6 m from the wall at a distance of 3 m below the wind girder.

The width of the spray is marginally greater than the wall flows illustrated in Figures 13 and 14. For a total flow rate of 550 m<sup>3</sup>/s this amount to 3-3.5m.

The overall spray dimensions for most of the drop below the wind girder are shown schematically in Figure 22.

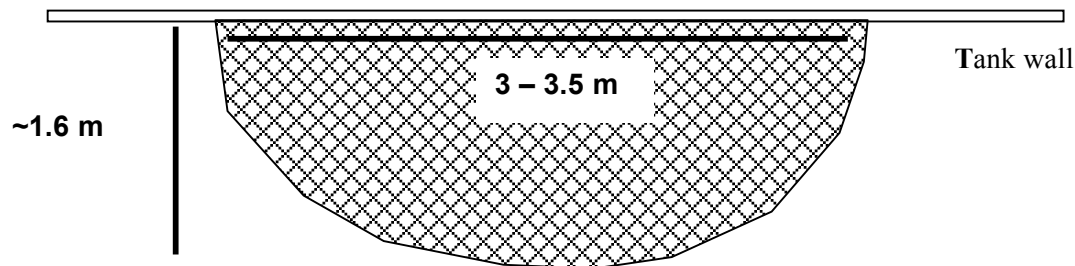


**Figure 22:** Schematic plan view of spray dimensions a few metres below the height of the wind girder.

The two features of this distribution of most significance are: i.) area - which defines the mass flux density of liquid and ii.) perimeter across which of air entrainment can occur i.e. not including the section adjacent to the wall.

Observation of sprays suggest that the area of the spray is around 4.5 m<sup>2</sup> and the perimeter over which entrainment is active is around 6 metres

### 3.5 SUMMARY OF RESULTS ON SPRAY GENERATION

1. Observations of water releases (where there are simultaneous overtopping and wall flows) suggest that the droplet size is variable, but typically fairly large (>5mm diameter) above the level of the wind-girder. Below the girder the characteristic size is reduced to a few millimetres.
2. A comparison between freely falling petrol and water sprays suggests that the relatively low surface tension of petrol increases the fineness of falling sprays.
3. Observations of sprays suggest that for the release that occurred from each of the vents at Buncefield the area of the spray a few metres below the wind-girder would have been around 4.5 m<sup>2</sup> and the perimeter over which entrainment was active would have been around 6 metres

## 4 CALCULATION OF VAPORISATION RATES

Computational Fluid Dynamics has been used to calculate the heat, mass and momentum transfer from a petrol cascade falling freely from a vent.

The following assumptions have been made:

1. Mass flows of petrol match the initial (550 m<sup>3</sup>/hr) and maximum values (960 m<sup>3</sup>/hr) during the incident.
2. The droplet diameter is 2mm below the wind girder. This is based on the best available evidence for the likely characteristic droplet size from observations of water and petrol sprays. Sensitivity studies showed that the output of most interest (volume flux driven by the spray) is very insensitive to the droplet size chosen.
3. The initial petrol and air temperatures are 14°C and 0°C respectively – taken from tank temperature records and weather records at the time of the incident.
4. The initial liquid composition (based on result of equilibrium thermodynamic analysis) is:

n-Butane (as a surrogate for all C4 hydrocarbons)	9.6% wt/wt
n-pentane (as a surrogate for all C5)	17.2 % wt/wt
n-hexane (as a surrogate for all C6)	16% wt/wt
n-decane (as a surrogate for all low volatility materials)	57.2% wt/wt
5. The initial cross section of the spray is assumed circular with an area of 4.5 m<sup>2</sup>. This approximately matches the area and entrainment perimeter of the sprays expected for the vent flow below the wind-girder.
6. A small initial (downward) vapour co-flow velocity has been imposed to stabilise the calculations. This has been subtracted from the results reported below.
7. Re-entrainment of hydrocarbons in an accumulated vapour cloud is not included.
8. Notes on the kinetic and thermodynamic sub-models employed are included as an appendix.



## 5

## RESULTS OF VAPORISATION MODELLING

As the spray falls it entrains (draws in) additional air. The downward volume flow of vapour driven by the liquid spray is of fundamental importance, as it determines the rate at which the vapour cloud grows near the source. Figure 23 shows how the induced volume flow per vent (of vapour and air) varied below the spray starting level.

Efficient dispersal of the liquid into a fine spray occurs at around the level of the wind-girder. As the spray falls below this level hydrocarbons are rapidly vaporised and fresh air is entrained into the spray. CCTV images of the area immediately adjacent to Bund A suggest that the vapour cloud depth for much of the release was around 4m - this is indicated on Figure 24.

Below the level of the top of the cloud (approximately 5m below the wind girder) the falling spray re-entrains contaminated air. This entrainment process does not increase the volume of the cloud - it simply increases the concentration of hydrocarbons. It is worth noting that the momentum of the downwash continues to increase as the spray penetrates the cloud and this is of significance in determining the vapour flow across and out of the bund

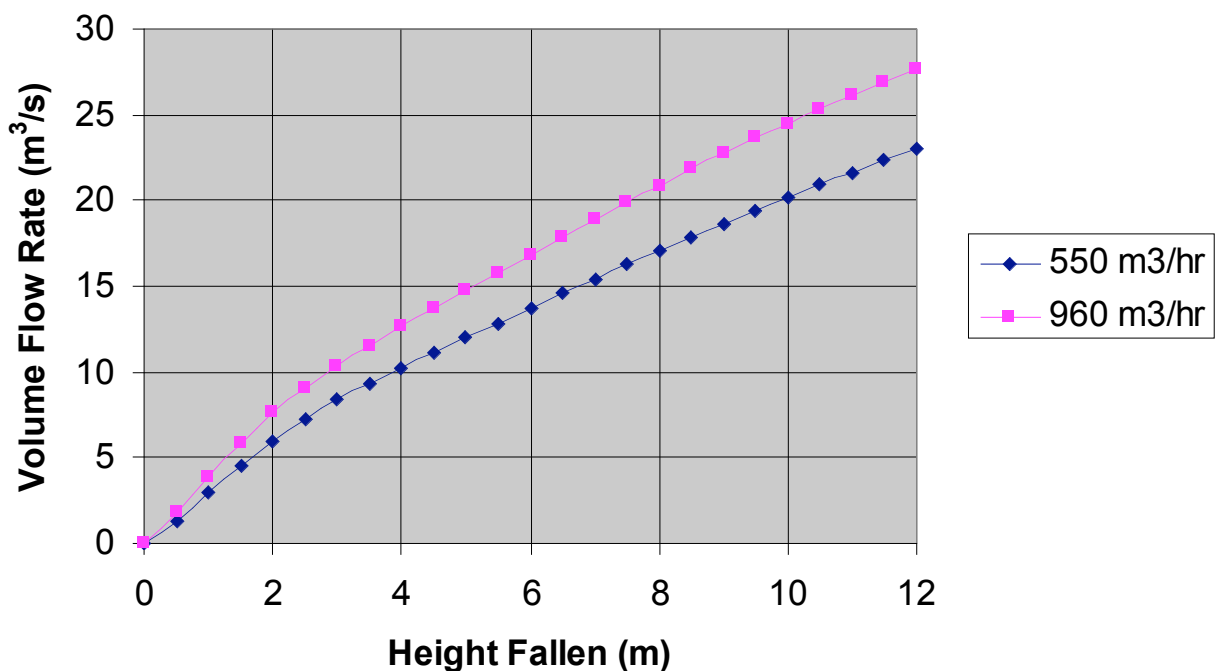


**Figure 23:** Variation of volume flow – vapour and air - (per vent) with height of fall

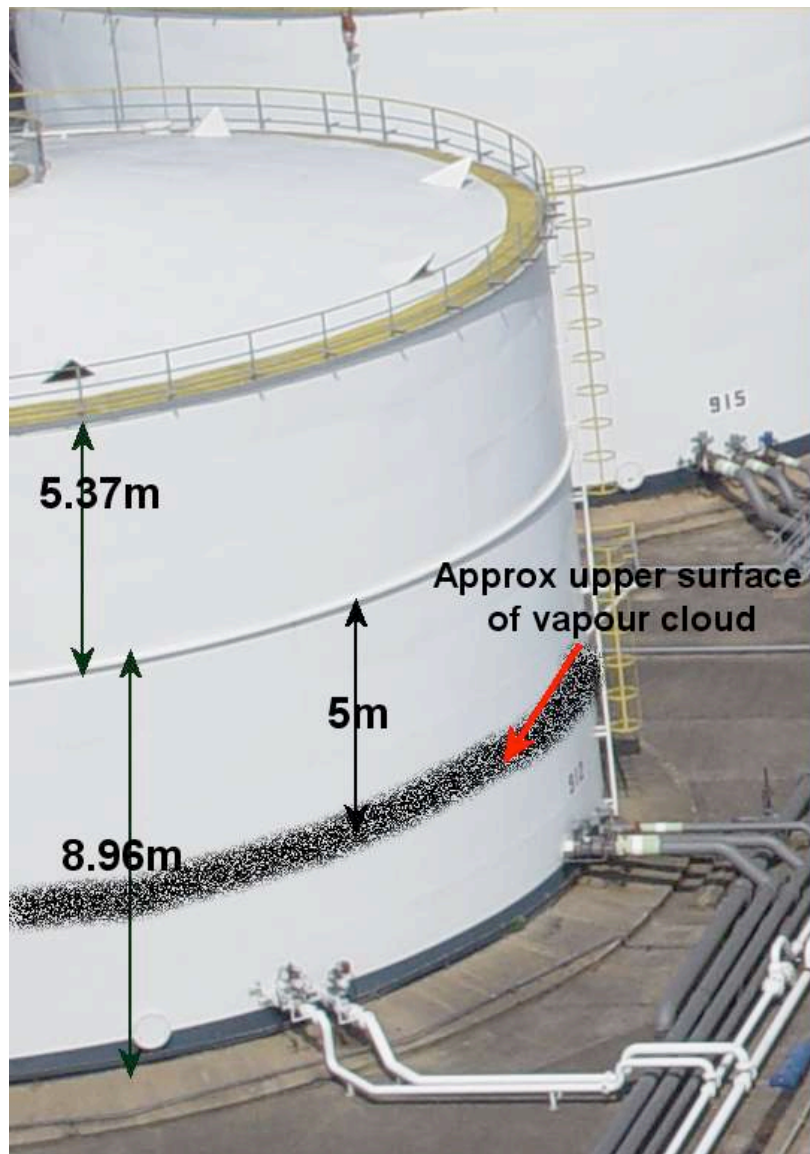


**Figure 24:** Approximate location of upper surface of vapour layer

Entrainment between the wind-girder level and the top of the vapour cloud corresponds to a fall of around 5 m. Figure 23 suggests an induced volume flow of around  $12 \text{ m}^3/\text{s}$  **per vent** for the lower release rate and  $15 \text{ m}^3/\text{s}$  for the higher rate. The total volume driven flow by releases from all eight vents in the tank would have been  $96 \text{ m}^3/\text{s}$  at the lower flow rate - rising to  $120 \text{ m}^3/\text{s}$  at the highest release rate.

The relative insensitivity of volume entrainment to the liquid release rate explains why the movement of the cloud visible in CCTV footage does not apparently speed up in the latter stages of the overflow – when the inflow rate increased.

The duration of the release was approximately 30 minutes (1800s). The total rates of vapour /air flow varies between  $96$  and  $120 \text{ m}^3/\text{s}$  and so the corresponding total volume production (at the source) must lie between  $173,000$  and  $215,000 \text{ m}^3$ . The plan area of the zone affected by combustion of the cloud was approximately  $110,000 \text{ m}^2$ . This implies that (without additional entrainment) the average cloud depth would have been approximately  $1.6 - 2 \text{ m}$  as the vapour spread in all directions away from Bund A.

CCTV records of the cloud suggest that in fact the average depth somewhat exceeded this level – indicating some entrainment into the cloud as it spread across the site. There is also strong evidence (from the level of sooting of exposed objects and overpressure sustained by the vapour combustion) that the vapour cloud was fuel rich close to the source and close to the stoichiometric ratio around the periphery of the cloud. This may also indicate significant entrainment into the spreading cloud. The development of the cloud is discussed in more detail in HSL Report CM/06/13.

Figure 25 shows the concentration of hydrocarbons in the high and low rate sprays.

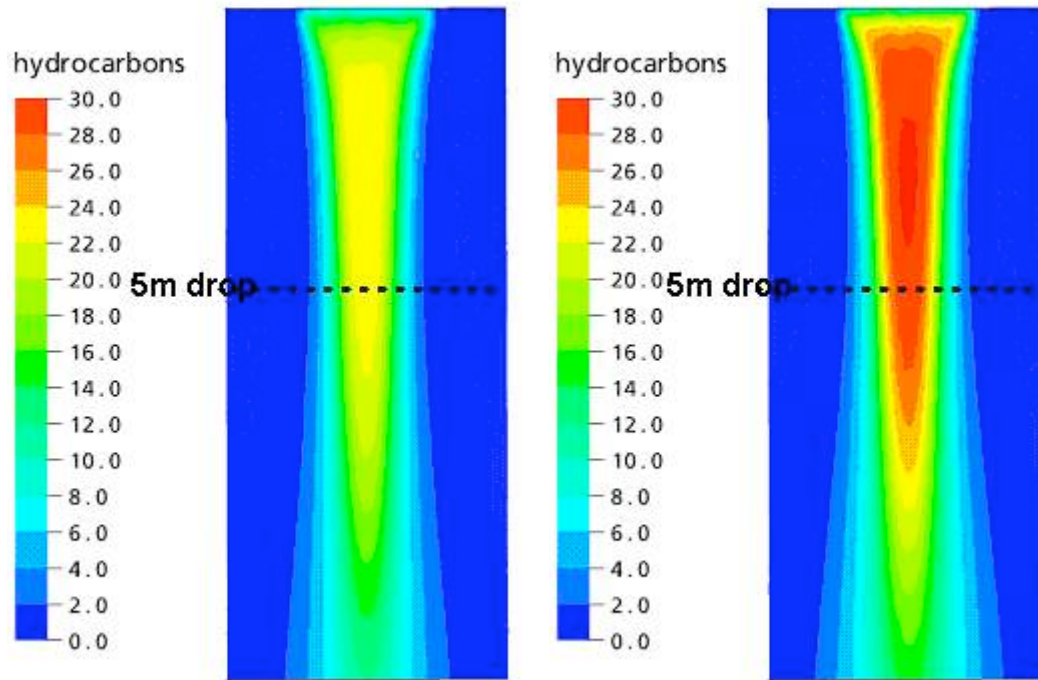


**Figure 25:** Contours of the total hydrocarbon mass fraction for the 550 m³/hr release rate (left) and 960 m³/hr release rate (right)

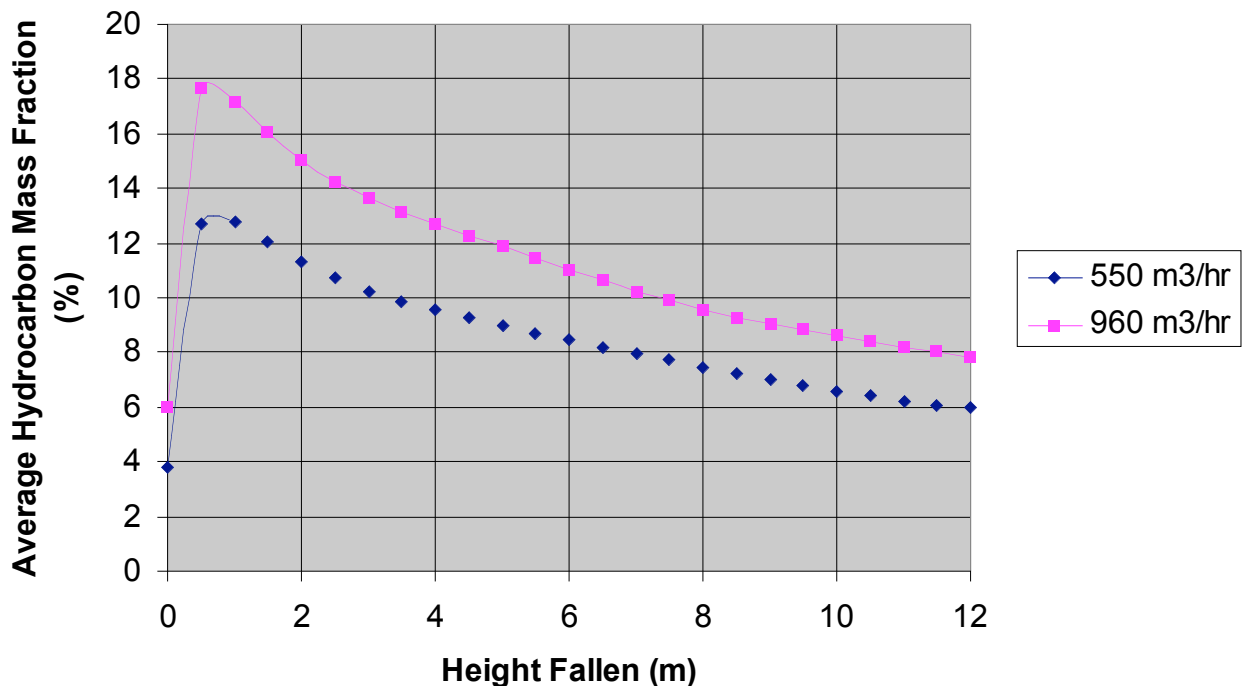
The maximum concentrations of hydrocarbons (on the axis of the spray) are well above the upper flammable limit.

Figure 26 shows the flow weighted average of hydrocarbon concentration as a function of spray drop.

The definition of a volume flux weighted average of a flow variable Y is the following.

$$\bar{Y}(z) = \frac{\iint Yv.dA}{\iint v.dA} \quad \text{where } v \text{ is the vertical velocity and the integration is carried across a}$$

horizontal plane at a distance z below the spray source. Such weighted averages are closely related to mass fluxes if Y is the mass concentration or heat flow if Y is the temperature.



**Figure 26:** Volume flux weighted average hydrocarbon concentration

Note: There is no re-entrainment of hydrocarbons in an accumulated vapour layer in this calculation

These average concentrations are in the flammable range but are not above the flammable limit - for a 5 m drop. In reality, for drops greater than 5 m the spray would start to re-entrain hydrocarbons. The combination of this re-entrainment and continued droplet evaporation is likely to lead to significant increases in average hydrocarbon content.

Further close contact between liquid and vapour will occur in the lower parts of the cascade (within the accumulated cloud), in the splash zone and at the surface of the liquid in the bund. Final temperatures and concentrations within liquid and vapour are likely to be very close to equilibrium values.

It is therefore interesting to calculate the hydrocarbon content of the vapour cloud if the induced air flow at 5m is allowed to reach equilibrium with all of the fuel released. For the low flow rate of fuel (550 m<sup>3</sup>/hr) the equilibrium concentration is around 13.7 % hydrocarbons (w/w) and the final temperature (of liquid and gas) is -8.4 °C. For the higher rate of fuel loss and induced air flow the corresponding figures are 16.3 % (w/w) and -7.1 °C. These concentrations are very close to and above the upper flammable limit respectively. These calculations assume 100% humidity but the ambient temperature is so low that enthalpy of condensation (and potentially freezing) of water has little effect on the overall energy balance. No heat transfer to bounding surfaces has been included.

Figures 26 and 27 show contour plots of temperature and line graphs of (volume flux weighted) average temperature as a function of spray drop. Even without allowing for the effect of cloud entrainment the average gas temperature falls below ambient. The humidity at the time of the release was very high and so any lowering of the gas temperature triggers condensation of droplets of water vapour – which is what makes the cloud visible. The possibility that aerosols

can be formed during droplet impacts followed by evaporation of fragments or by a condensation process are examined in HSL CM/06/13. Neither mechanism appears capable of generating significant amounts of droplets fine enough to form a persistent cloud.

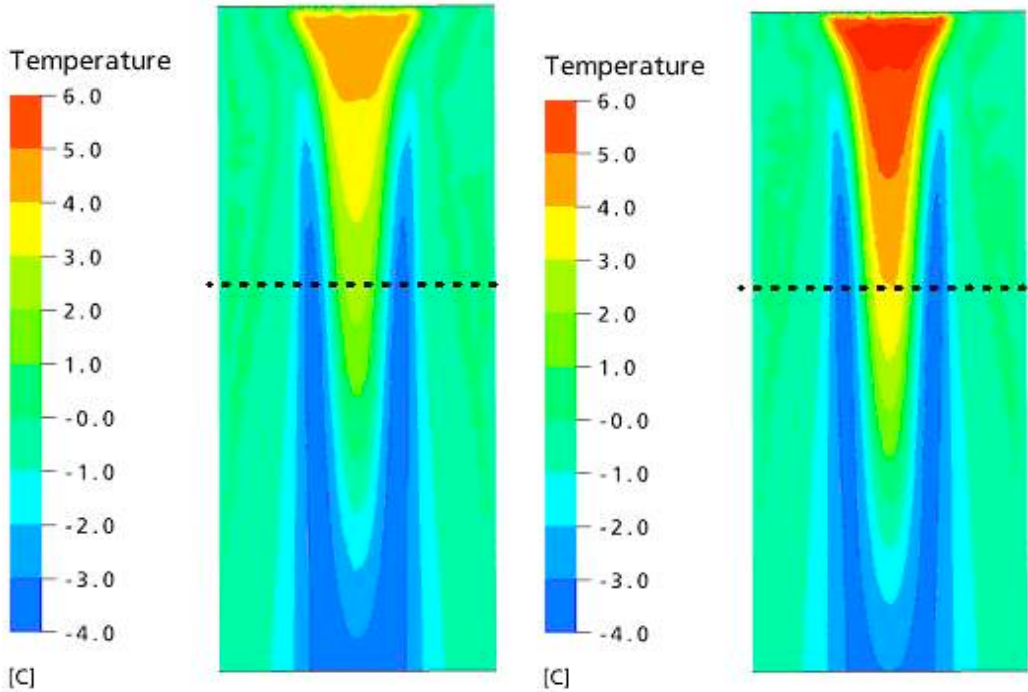


**Figure 27:** Contours of the vapour temperature for the 550 m<sup>3</sup>/hr release rate (left) and 960 m<sup>3</sup>/hr release rate (right)

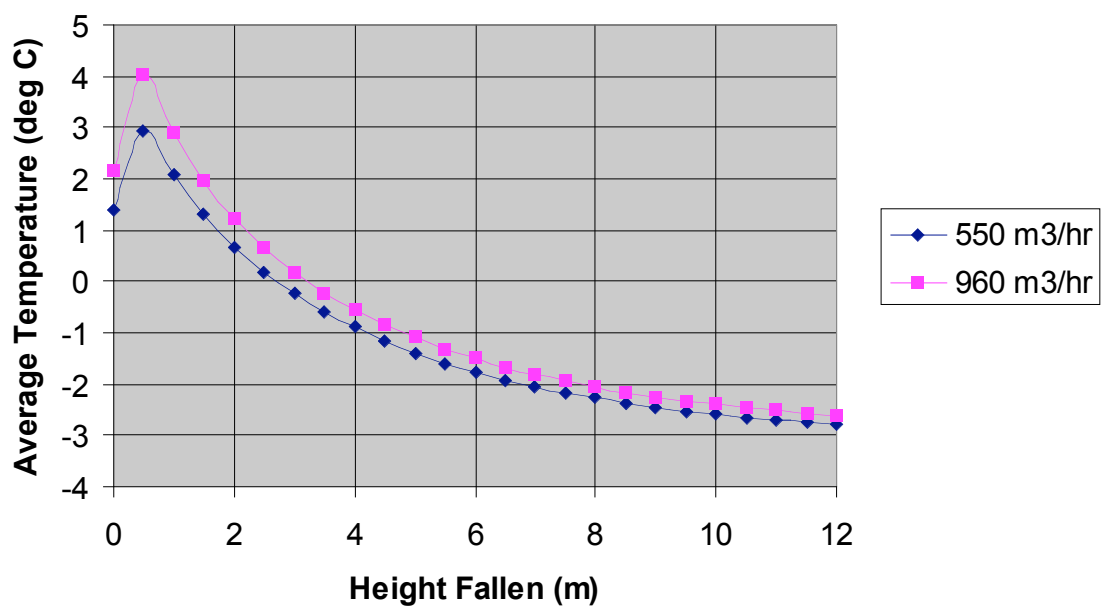


**Figure 28:** Decline in average (flow weighted) gas temperature  
 Note: There is no re-entrainment of hydrocarbons in an accumulated vapour layer in this calculation

## 6 SUMMARY OF CHARACTERISTICS OF VAPOUR (AND RESIDUAL LIQUID) PRODUCED BY FALLING SPRAYS

When the cascade is modelled as an assembly of 2 mm droplets, the hydrocarbon vapour concentration as the liquid cascade enters the vapour cloud at the base of the tank is approximately 70% of the equilibrium value. Further close contact between liquid and vapour will occur in the lower parts of the cascade (within the accumulated cloud), in the splash zone and at the surface of the liquid in the bund. Final temperatures and concentrations within liquid and vapour are likely to be very close to equilibrium values.

The following estimates of vapour and liquid temperatures and concentrations are therefore based on equilibrium calculations.

### Initial liquid composition

n-butane (as a surrogate for all C4 hydrocarbons)	9.6% wt/wt
n-pentane (as a surrogate for all C5)	17.2 % wt/wt
n-hexane (as a surrogate for all C6)	16% wt/wt
n-decane (as a surrogate for all low volatility materials)	57.2% wt/wt

### 6.1 LOW LIQUID OVERFLOW RATE (550 M<sup>3</sup>/HR)

Rate at which vapour added to cloud 96 m<sup>3</sup>/s

Final vapour and liquid temperature -8.5 C.

#### Vapour composition

n-Butane (as a surrogate for all C4 hydrocarbons)	6.0 % wt/wt
n-pentane (as a surrogate for all C5)	6.1 % wt/wt
n-hexane (as a surrogate for all C6)	2.06% wt/wt
Total hydrocarbons	14.17 % wt/wt

#### Residual liquid composition

n-butane (as a surrogate for all C4 hydrocarbons)	2.4% wt/wt
n-pentane (as a surrogate for all C5)	11.5 % wt/wt
n-hexane (as a surrogate for all C6)	16.3 % wt/wt
n-decane (as a surrogate for all low volatility materials)	69.6 % wt/wt

### 6.2 HIGH LIQUID OVERFLOW RATE (960 M<sup>3</sup>/HR)

Rate at which vapour added to cloud 120 m<sup>3</sup>/s

Final vapour and liquid temperature -7.2 C.

#### Vapour composition

n-Butane (as a surrogate for all C4 hydrocarbons)	7.6 % wt/wt
n-pentane (as a surrogate for all C5)	6.9 % wt/wt
n-hexane (as a surrogate for all C6)	2.17% wt/wt
Total hydrocarbons	16.7 % wt/wt

#### Residual liquid composition

n-butane (as a surrogate for all C4 hydrocarbons)	3 %	wt/wt
n-pentane (as a surrogate for all C5)	12.7 %	wt/wt
n-hexane (as a surrogate for all C6)	16.5 %	wt/wt
n-decane (as a surrogate for all low volatility materials)	67.7 %	wt/wt

## 7 CONCLUSIONS

1. Observations of water releases (where there are simultaneous overtopping and wall flows) suggest that the droplet size is variable, but typically fairly large ( $>5\text{mm}$  diameter) above the level of the wind-girder. Below the girder the characteristic size is reduced to a few millimetres.
2. A comparison between freely falling petrol and water sprays suggests that the relatively low surface tension of petrol increases the fineness of falling sprays.
3. Observations of sprays suggest that for the release that occurred from each of the vents at Buncefield the area of the spray a few metres below the wind-girder would have been around  $4.5\text{ m}^2$  and the perimeter over which entrainment was active would have been around 6 metres
4. The height difference between the wind-girder level and the top of the vapour cloud corresponds to a fall of around 5 m. CFD calculations of the rate of air entrained by the liquid cascade suggests an induced volume flow of around  $12\text{ m}^3/\text{s}$  **per vent** for a total overflow rate of  $550\text{ m}^3/\text{hour}$ . The total volume driven flow by releases from all eight vents in the tank would have been  $96\text{ m}^3/\text{s}$ .
5. The vapour volume flux rises to  $15\text{ m}^3/\text{s}$  for a total overflow rate of  $960\text{ m}^3/\text{hour}$  (the highest rate of overfilling during the Buncefield incident). The total volume driven flow by releases from all eight vents in the tank in this case would have been  $96\text{ m}^3/\text{s}$ .
6. The rate of vapour production is insensitive to the droplet size.
7. When the cascade is modelled as an assembly of  $2\text{ mm}$  droplets, the hydrocarbon vapour concentration as the liquid cascade enters the vapour cloud at the base of the tank is approximately 70% of the equilibrium value. Further close contact between liquid and vapour will occur in the lower parts of the cascade (within the accumulated cloud), in the splash zone and at the surface of the liquid in the bund. Final temperatures and concentrations within liquid and vapour are likely to be very close to equilibrium values.



The Computational Fluid Dynamics (CFD) modelling of the petrol spray has been undertaken using the commercial CFD code, CFX. The model solves equations for both the droplets and the surrounding air-vapour mixture and models the two-way interaction of mass, momentum and energy between the droplets and gas.

Figure A1 shows the flow configuration studied. Petrol droplets are injected through a circular area in the top of the domain with a small coflow of air. As the droplets fall under gravity, they drag some air with them. This entrainment causes some air to be drawn into the flow domain through the open sides. As the petrol droplets fall they also evaporate. This has a cooling effect due to the absorption of latent heat. The heat transfer between the cooling droplets and the surrounding gas is accounted for in the model.

The modelled droplets are composed of a simplified petrol mixture of butane, pentane, hexane and decane. These four components have different vapour pressures and so evaporate at different rates. The vapour pressures are also functions of the local temperature. Figure A1 shows the decrease in butane concentration of the droplets as they fall through the air. Once the flow has become established (after a few metres drop), the droplets in the core become surrounded by gas which is rich in butane whereas due to the entrainment of fresh air the droplets on the periphery are surrounded by clean air. This leads to different concentration gradients in the core and periphery of the spray and the difference in droplet butane concentrations (blue and green lines) shown in the Figure A1.

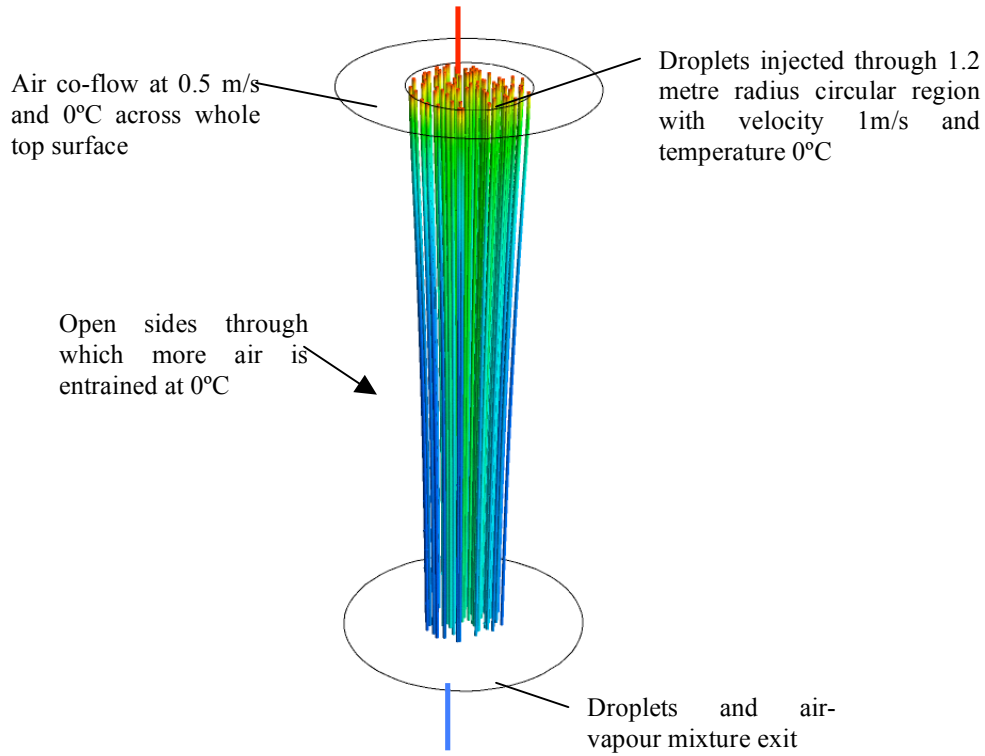


**Figure A1:** The CFD model showing sample droplet trajectories coloured with the butane mass fraction.

The gas phase is modelled using an Eulerian treatment with conservation equations solved for mass, momentum, energy, two turbulence model equations and four additional equations for the mass fractions of butane, pentane, hexane and decane vapour. For the droplets, a particle tracking or ‘Lagrangian’ approach is used.

The temperature of the droplets is affected by convective heat transfer with the air, and latent heat transfer associated with evaporation. The modelled convective heat transfer,  $Q_c$ , is a function of an empirical Nusselt number coefficient:

$$Q_c = \pi d \lambda_g Nu (T_g - T_d)$$

where subscripts  $g$  and  $d$  refer to the continuum gas phase and the droplet respectively,  $\lambda$  is the thermal conductivity,  $d$  is the droplet diameter and  $T$  the temperature. The Nusselt number,  $Nu$ , is calculated from the empirical formula:

$$Nu = 2 + 0.6 Re^{1/2} \sigma^{1/3}$$

and the Prandtl number,  $\sigma$ , is defined as:

$$\sigma = \frac{\mu_g c_{p,g}}{\lambda_g}$$

Terms  $\mu_g$  and  $c_{p,g}$  are the dynamic viscosity and specific heat capacity of continuum gas phase. The Reynolds number is calculated from the slip velocity:

$$Re = \frac{\rho_g (|\mathbf{u}| - |\mathbf{u}_d|) d}{\mu_g}$$

where  $|\mathbf{u}|$  is the magnitude of the gas mixture velocity and  $|\mathbf{u}_d|$  the magnitude of the droplet velocity.

The mass transfer rate due to evaporation,  $\dot{m}$ , is governed by the following equation:

$$\dot{m} = \min \left[ \pi d D_g Sh \frac{W_c}{W_g} \ln \left( \frac{1 - X_c}{1 - X_g} \right), 0 \right]$$

where subscript  $c$  refers to the gas-phase properties of the component evaporating and subscript  $g$  to the properties of the gas continuum mixture surrounding the droplet,  $W$  is the relative molecular masses,  $d$  is the droplet diameter,  $D$  is the dynamic diffusivity (with units kg/m/s),  $X_g$  is the equilibrium molar fraction and  $X_c$  the actual molar fraction. The  $\min$  function is used to clip  $\dot{m}$  so that no condensation is modelled, only evaporation. When the concentration of gas surrounding the droplet reaches the equilibrium concentration ( $X_c = X_g$ ) the mass transfer rate falls to zero ( $\dot{m} = 0$ ). The terms  $X_c$  and  $X_g$  are calculated as follows:

$$X_c = \frac{\gamma_c \rho_g}{W_c C_g} \quad X_g = x_d \frac{P_c^{sat}}{P}$$

where  $\gamma$  is the mass fraction,  $C$  is the molar concentration (found from the ideal gas law,  $C = P / R_u T$ ),  $P_c^{sat}$  is the saturation vapour pressure for the component evaporating,  $P$  is the total pressure in the gas mixture and  $x_d$  is the molar fraction of the species evaporating in the droplet. The presence of  $x_d$  in the model equation is necessary for the model to be consistent with Raoult's Law.

The expression for the molar fraction,  $X_c$ , can be expanded as follows:

$$X_c = \frac{\gamma_c \rho_g}{W_c C} = \frac{\left[ \frac{m_c}{m_c / N_c} \right] \left[ \frac{m_g}{N_g / Vol} \right]}{\left[ \frac{m_c}{m_c / N_c} \right] \left[ \frac{m_g}{N_g / Vol} \right]} = \frac{N_c}{N_g}$$

where  $m$  is the mass,  $N$  is the number of moles and  $Vol$  a unit volume.

The Sherwood number,  $Sh$ , is calculated from:

$$Sh = 2 + 0.6Re^{1/2} Sc^{1/3}$$

and the Schmidt number,  $Sc$ , from:

$$Sc = \frac{\mu_g}{\rho_c D_c}$$

The saturation vapour pressure for each component is determined from the Antoine equation:

$$P^{sat} = P^{ref} \exp\left(A - \frac{B}{T + C}\right)$$

where  $T$  is the temperature,  $P^{ref}$  is a reference pressure and  $A$ ,  $B$  and  $C$  are empirical coefficients which are different for each component evaporating.



# Buncefield investigation

## Liquid flow and vapour production

This report on the liquid flow from the overfilled tank leading to the formation of flammable vapour in the Buncefield Incident was prepared for the HSE incident investigation. The purpose of the work was to provide a connection between the loss of containment and the formation of a flammable vapour cloud. Practical and numerical investigations have demonstrated that the bulk of fuel vaporisation and entrainment of air occurred during the cascading of fuel from the top of the tank into the bund.

The work involved the construction of a full scale replica of a section of top of the tank involved at Buncefield and also a full height section of the tank wall. Liquid flow experiments were carried out. The overall liquid flow results in a relatively fine spray, with droplets a few millimetres in diameter. Numerical analysis of heat, mass and momentum transfer (between droplets in the fuel cascade and the air that surrounds them) has shown that the fuel cascade drives a significant downward flow of air. The air is contaminated by high concentrations of light hydrocarbons and is cooled. Final temperatures and concentrations within liquid and vapour are likely to be very close to equilibrium values.

This report and the work it describes were funded by the Health and Safety Executive (HSE). Its contents, including any opinions and/or conclusions expressed, are those of the authors alone and do not necessarily reflect HSE policy.